

A Validated Quantitative Assay to Detect Occult Micrometastases by Reverse Transcriptase-Polymerase Chain Reaction of Guanylyl Cyclase C in Patients with Colorectal Cancer

Stephanie Schulz,¹ Terry Hyslop,¹ Janis Haaf,¹ Christine Bonaccorso,¹ Karl Nielsen,¹ Matthew E. Witek,¹ Ruth Birbe,² Juan Palazzo,² David Weinberg,³ and Scott A. Waldman¹

Abstract Purpose: Guanylyl cyclase C (GCC), a receptor for bacterial diarrheagenic enterotoxins, may be a prognostic and predictive marker to detect occult micrometastases in patients undergoing staging for colorectal cancer. However, quantification of GCC expression in tissues by the quantitative reverse transcription-PCR (qRT-PCR) has not undergone analytic and clinicopathologic validation.

Experimental Design: A technique to quantify GCC mRNA in tissues employing RT-PCR was developed and validated employing external calibration standards of RNA complementary to GCC.

Results: GCC qRT-PCR exhibited reaction efficiencies >92%, coefficients of variations <5%, linearity >6 orders of magnitude, and a limit of quantification of >25 copies of GCC cRNA. This assay confirmed that GCC mRNA was overexpressed by colorectal tumors from 41 patients, which correlated with increased GCC protein quantified by immunohistochemistry. Analyses obtained with 164 lymph nodes from patients free of cancer and 15 nodes harboring metastases established a threshold for metastatic disease of ~200 GCC mRNA copies/ μ g total RNA, with a sensitivity of 93% and specificity of 97%. GCC mRNA above that threshold was detected in 76 of 367 (~21%) nodes free of disease by histopathology from 6 of 23 (26%) patients, suggesting the presence of occult micrometastases.

Conclusions: Quantifying GCC mRNA in tissues by RT-PCR employing external calibration standards is analytically robust and reproducible, with high clinicopathologic sensitivity and specificity. This validated assay is being applied to ~10,000 lymph nodes in a prospective trial to define the sensitivity of GCC qRT-PCR for staging patients with colorectal cancer.

Colorectal cancer is the third leading cause of cancer and the second leading cause of cancer-related mortality in the United States (1). The single most important prognostic and predictive determinant for the management of affected patients is the presence of metastatic tumor cells in regional lymph nodes (2, 3). Indeed, patients with metastases to regional lymph nodes have an increased risk of developing recurrent disease

and receive adjuvant chemotherapy with well-defined efficacy (1–4). In contrast, patients with disease confined to the bowel wall generally have a reduced risk of developing recurrent disease and receive conservative management consisting of surgery and postoperative surveillance (1–5). However, up to 35% of patients with disease ostensibly confined to the intestine subsequently develop metastatic disease, presumably reflecting occult micrometastases in regional lymph nodes and other tissues that escape detection at the time of staging (6–8). Understaging likely reflects the limitations of current paradigms, including inadequate lymph node sampling (9, 10), inadequate sampling of tissues available for analysis (6–8), and limitations in analytic sensitivity of routine histopathology (6–8, 11). Unfortunately, failure to identify micrometastases can result in undertreatment of patients who might otherwise benefit from chemotherapy (6, 8, 9, 12).

These considerations underscore the unmet need for approaches to more accurately stage patients with colorectal cancer. In that context, an emerging paradigm in molecular diagnostics involves the detection of rare cancer cells employing sensitive amplification techniques and specific tumor markers (6–8). Indeed, the reverse transcription-PCR (RT-PCR) is a sensitive and specific method to quantify the expression of rare mRNA molecules in nucleic acids extracted from tissue

Authors' Affiliations: Departments of ¹Pharmacology and Experimental Therapeutics and ²Pathology, Anatomy, and Cell Biology, Thomas Jefferson University, and ³Division of Gastroenterology, Department of Medicine, Fox Chase Cancer Center, Philadelphia, Pennsylvania

Received 4/7/06; revised 5/15/06; accepted 5/25/06.

Grant support: NIH CA79663 and CA95026 and Targeted Diagnostics and Therapeutics, Inc.

The costs of publication of this article were defrayed in part by the payment of page charges. This article must therefore be hereby marked *advertisement* in accordance with 18 U.S.C. Section 1734 solely to indicate this fact.

Note: S.A. Waldman is the Samuel M.V. Hamilton Professor of Medicine of Thomas Jefferson University.

Requests for reprints: Scott A. Waldman, 132 South 10th Street, 1170 Main, Philadelphia, PA 19107. Phone: 215-955-6086; Fax: 215-955-7006; E-mail: Scott.Waldman@jefferson.edu.

©2006 American Association for Cancer Research.
doi:10.1158/1078-0432.CCR-06-0865

specimens (13–16). This technique overcomes key limitations in current staging paradigms, including inadequate tissue sampling, because RNA can be extracted from the entire specimen and sampled analytically. Moreover, RT-PCR can detect a single cancer cell in 10^6 to 10^7 normal cells, improving detection sensitivities >4 orders of magnitude compared with histopathology, which detects a single cancer cell in $\sim 10^2$ normal cells (12–16).

Although amplification technologies have provided highly sensitive methods for cancer cell enumeration, the availability of tumor markers with sensitivities and specificities sufficient to reliably quantify occult colorectal cancer cells and to which amplification technologies can be applied have lagged (14). In that regard, guanylyl cyclase C (GCC) is the intestine-specific member of the particulate family of guanylyl cyclases (17). GCC is the receptor for the endogenous peptides guanylin and uroguanylin and diarrheagenic bacterial heat-stable enterotoxins. Canonical signaling by this family of proteins involves ligand-induced accumulation of intracellular cyclic guanosine 3',5'-monophosphate, which in intestinal epithelial cells regulates ionic conductances and fluid and electrolyte secretion, manifesting as diarrhea. Of significance, GCC is selectively expressed in apical membranes of intestinal epithelial cells from the duodenum to the rectum but not in tissues or tumors originating outside the gastrointestinal tract (18–20). Further, this receptor continues to be expressed after normal epithelial cells undergo neoplastic transformation and become colorectal cancer cells (19, 20). Moreover, GCC expression has been identified in every primary and metastatic colorectal tumor obtained from patients regardless of tumor grade or anatomic location (19–22). Thus, GCC may fulfill the criteria for a sensitive and specific prognostic and predictive marker for identifying occult colorectal micrometastases (12). Indeed, in a retrospective analysis, detection of GCC expression by qualitative RT-PCR in lymph nodes free of metastases by histopathology was highly associated with the development of recurrent colorectal cancer (23).

The foregoing suggests that quantitative RT-PCR (qRT-PCR) for GCC might enumerate clinically significant occult tumor cells in lymph nodes of patients undergoing staging for colorectal cancer. In that context, GCC qRT-PCR is being examined in a multicenter prospective clinical trial to accurately identify occult micrometastases that predict clinical outcomes in patients with colorectal cancer (12). Of significance, few, if any, molecular markers have undergone rigorous analytic and clinicopathologic validation for detecting rare tumor cells in otherwise normal tissues by qRT-PCR. Here, analytic and clinicopathologic validation of the assay for quantifying GCC mRNA by RT-PCR employed in that prospective clinical trial is described. The assay, which quantifies GCC mRNA in tissues by comparison with a standard curve amplifying RNA complementary to GCC, exhibits high analytic sensitivity, with a lower limit of quantification of 25 copies of GCC mRNA, and is robust, with a coefficient of variation (CV) of <5%. This assay confirmed that GCC is overexpressed by primary colorectal tumors compared with matched normal adjacent mucosa (18). Moreover, this assay exhibited a nominal sensitivity of 93% when applied to lymph nodes harboring colorectal metastases identified by histopathology (true positives) and a specificity of >97% employing lymph nodes from patients who did not have colorectal cancer (true negatives). Importantly, GCC qRT-

PCR revealed that 76 of 367 ($\sim 21\%$) lymph nodes free of tumor cells by histopathology from 6 of 23 (26%) patients with colorectal cancer may harbor occult micrometastases.

Materials and Methods

Surgical samples. Tissue samples were obtained from patients undergoing surgery at Thomas Jefferson University Hospital under a protocol approved by the institutional review board (control 01.0823). A pathologist (R.B. or J.P.) reviewed all H&E-stained slides to confirm the diagnosis and ensure the presence of representative tissues. All diagnoses in this study were established using current standard criteria, and specimens included 10 small intestines, 85 normal colonic mucosa, 26 adenomas, 63 colorectal adenocarcinomas, and 546 lymph nodes. Of 41 colorectal cancer patients, 23 (56%) were female and 13 (44%) were male, with an average age of 68 years (31–95 years). In these patients, tumors were recovered from the cecum (7%), ascending (37%), transverse (7%), descending (2%), sigmoid (35%), and rectum (12%). The majority (80%) of tumors were moderately differentiated, with a minority either well (10%) or poorly (10%) differentiated. Specimens of colon tumor and histologically normal mucosa were dissected free of underlying muscle and fat. Colonic lymph nodes were dissected using a clean set of surgical instruments and bisected. Half of each lymph node was submitted for standard histopathologic examination. Tonsils were obtained from children undergoing routine tonsilectomy. All samples were either snap-frozen or frozen in RNA-Later (Ambion, Austin, TX).

RNA extraction. RNA was extracted from tissues by a modification of the acid guanidinium thiocyanate-phenol-chloroform extraction method (19, 23). Briefly, individual tissues were pulverized in 1.0 mL Tri-Reagent (Molecular Research Center, Cincinnati, OH) with 12 to 14 sterile 2.5-mm zirconium beads in a bead mill (Biospec, Bartlesville, OK) for 1 to 2 minutes. Phase separation was done with 0.1 mL bichloropropane, and the aqueous phase was reextracted with 0.5 mL chloroform. RNA was precipitated with isopropanol and washed with 75% ethanol. Linear acrylamide (50 μg) was included when lymph nodes were <1 mm in diameter. Air-dried RNA was dissolved in water, concentration determined by spectrophotometry, and stored at -80°C .

Synthesis of cRNA standards. Bluescript plasmids containing ~ 1.5 kb of the human GCC cDNA, corresponding to the extracellular ligand-binding domain (Bluescript SK, Stratagene, La Jolla, CA), or full-length human β -actin cDNA (Bluescript KS, Stratagene) were linearized with *Bam*HI or *Xho*I, respectively. Linearized plasmids were used as templates for *in vitro* transcription (T7 Ribomax kit, Promega, Madison, WI). Template DNA was removed by DNase I digestion, and the *in vitro* transcripts were purified on RNeasy columns (Qiagen, Valencia, CA). Concentrations of cRNA were determined by spectrophotometry, and GCC and β -actin copy number was calculated. Standards were diluted to 1×10^9 copies/ μL and stored at -80°C .

Quantitative RT-PCR. The EZ RT-PCR kit (Applied Biosystems, Foster City, CA) was employed to amplify GCC mRNA from total RNA in a 50 μL reaction. Optical strip tubes were used for all reactions, which were conducted in an ABI 7000 Sequence Detection System (Applied Biosystems). In addition to the kit components [50 mmol/L Bicine (pH 8.2); 115 mmol/L KOAc; 10 $\mu\text{mol/L}$ EDTA; 60 nmol/L ROX; 8% glycerol; 3 mmol/L Mg(OAc)₂; 300 $\mu\text{mol/L}$ each of dATP, dCTP, and dGTP; 600 $\mu\text{mol/L}$ dUTP; 0.5 unit uracil N-glycosylase; 5 units rTth DNA polymerase], the reaction master mix contained 900 nmol/L each of forward (ATTCTAGTGGATCTTTTCAATGACCA) and reverse (CGTCAGAACAAAGGACATTTTTCAT) primers, 200 $\mu\text{mol/L}$ Taqman probe (FAM-TACTTGGAGGACAATGTCACAGCCCCCTG-TAMRA), and 1 μg RNA template or a known amount of cRNA standard. β -Actin was amplified using similar conditions, except that forward (CCACTGTGCCCATCTACG) and reverse (AGGATCTTCATGAGGTAGT-CAGTCAG) primers were 300 nmol/L each, whereas the Taqman probe

(FAM-ATGCCX(X(TAMRA)-CCCCATGCCATCCTGCGTp) was 200 $\mu\text{mol/L}$. The thermocycler program employed included 50°C \times 2 minutes, 60°C \times 30 minutes, 95°C \times 5 minutes for reverse transcription and 45 cycles of 94°C \times 20 seconds and 62°C \times 1 minute for PCR. Serial dilutions provided concentrations of 25, 50, 100, 2×10^2 , 2×10^3 , 2×10^4 , 2×10^5 , and 2×10^6 from the stock 1×10^9 copies/ μL . Standard reactions were done at least in duplicate and results were averaged; where appropriate, data are representative of at least three independent experiments. For patient specimens, GCC copy number was not routinely normalized to a housekeeping gene, reflecting the heterogeneity of contribution of epithelial and stromal cells to different specimens; the variability of expression of housekeeping genes in different cells, tissues, and patients; and the general acceptance of normalization to amount of total RNA analyzed (14, 24–26). Specimens yielding $< 2 \times 10^3$ copies of β -actin mRNA/ μg total RNA were deemed insufficient and omitted from further analysis.

Antibodies. A 19-residue peptide, corresponding to the structurally unique, antigenically active COOH terminus of human GCC (residues 1,032-1,050), was conjugated to keyhole limpet hemocyanin and used to immunize rabbits (Alpha Diagnostic International, San Antonio, TX; ref. 18). Sera with the highest titer by ELISA were used for further purification. The immunizing peptide was coupled to immobilized iodoacetyl (SulfoLink, Pierce, Rockford, IL) through a NH_2 -terminal cysteine residue. Peptide was coupled and antisera were purified according to the manufacturer's protocol. Fractions eluting with low [0.2 mol/L glycine/150 mmol/L NaCl (pH 0.2)] or high [0.2 mol/L triethylamine/150 mmol/L NaCl (pH 11.5)] pH buffer were neutralized, pooled, and dialyzed against PBS.

Immunohistochemistry. GCC immunohistochemistry was done as described (18). Briefly, sections (5 μm) of formalin-fixed, paraffin-embedded tissues were mounted on Superfrost Plus-charged slides. Routine deparaffinization from xylene to 95% alcohol was done on a Leica autostainer (Leica, Inc., Deerfield, IL). This process included a 30-minute methanolic peroxide step to block endogenous peroxidase activity. Slides were then rehydrated and antigen recovery was done at 70% power in a 1,050 W microwave oven (model EM-F3400, Sanyo, Chatsworth, CA) in EDTA buffer (pH 8.0). Slides were microwaved for two intervals of 5 minutes each, with replenishment of evaporated buffer between exposures. After a 30-minute cooling period, slides were washed in deionized water and placed in PBS for 5 minutes. Immunostaining was conducted employing a DAKO autostainer (model LV-1, DAKO Corp., Carpinteria, CA). Slides were incubated for 15 minutes each with avidin and blocking solutions (Vector Laboratories, Burlingame, CA) followed by primary antibody (1:200) for 60 minutes. After a PBS wash, biotinylated goat anti-rabbit IgG was applied to slides for 30 minutes followed by avidin-biotin complex (Vector Laboratories) for 30 minutes. After another PBS wash, slides were incubated for 5 minutes in 3,3'-diaminobenzidine solution (DAKO), washed in deionized water, counterstained with Harris hematoxylin (SurgiPath, Richmond, IL), and dehydrated with xylene before mounting. In some experiments, purified rabbit antibodies were preincubated with the immunizing peptide before immunostaining to confirm that staining reflected specific interaction with GCC. Apical membrane staining was scored by two pathologists using a modified McCarty scale of +1 to +3 representing intensity of staining (27).

Statistical analyses. Mixed-effects linear models with random slope and intercepts per run within plate were used to assess linearity and variability of the assay standards across concentrations. Model variations included both fixed and random nominal effects of concentration to assess intra-assay and interassay variability. This variability is reported as the intra-assay and interassay CV defined as $100 \times (\text{SD} / \text{mean})$. Amplification slope efficiency is defined based on the slope of threshold cycle (C_t) versus log of concentration for each run: $\text{efficiency} = 10^{(-1 / \text{slope})} - 1$. Limit of detection of the assay is the lowest concentration at which fluorescence could be detected in $>95\%$ of the samples, whereas limit of quantitation is the lowest concentration at which fluorescence could be detected consistently in all samples.

Paired tumor and normal adjacent tissue samples were compared employing the Wilcoxon signed-rank test, the nonparametric equivalent of a paired t test, used here to determine overexpression or underexpression of GCC in paired patient samples. Associations of GCC copy number in tumor and normal adjacent tissue with Dukes stage, differentiation status, T stage, N stage, M stage, and grade of tumors were examined employing the Kruskal-Wallis test. This is a nonparametric equivalent of a one-way ANOVA, testing for differences in median gene expression across the categories investigated. The exact Kruskal-Wallis test was used to test the association of GCC apical staining intensity with tissue type. The "exact" form of the nonparametric one-way ANOVA is used due to small sample sizes in some categories of staining intensity. GCC expression was compared in tumors and matched normal adjacent tissue by quantifying differences in copy number and by the ratio of GCC in tumor and normal adjacent tissue (fold change). The sensitivity and specificity to detect tumor cells in lymph nodes employing GCC RT-PCR was determined employing lymph nodes harboring metastases detected by histopathology (true positives) and lymph nodes from patients with no evidence of colorectal cancer (true negatives). This analysis and the selection of the optimal cut point were completed using receiver operating characteristic analyses using logistic regression models followed by classification table analyses. In all analyses, two-sided tests were used and $P < 0.05$ was considered statistically significant.

Results

Validation of GCC cRNA calibration curve. Forward and reverse primers were designed that specifically recognize exons 6 and 7 of GCC, respectively, and produce a small (84-bp) amplicon. The 3' end of the forward primer lies across the exon/intron 6 boundary, effectively eliminating genomic DNA as a template for amplification. Purified cRNA standards, corresponding to the structurally unique extracellular ligand-binding domain of GCC, of defined concentrations, were employed to develop a calibration curve to quantify GCC mRNA in tissues. The performance characteristics of this assay were evaluated employing a series of replicate runs in which two standard curves, each derived from an independent master mix, were generated each day for 5 days for a total of 10 curves. At copy levels of ≤ 100 , samples were run in replicates of five, whereas all other standards (2×10^2 - 2×10^6 copies) were run in triplicate. Amplification reactions were exponential and there was an inverse relationship between initial cRNA copy number and C_t quantified by the change in fluorescence [$\Delta R(x)$; Fig. 1A]. Linear mixed model analysis of the relationship between C_t number and calibrator concentration (Fig. 1B) yielded an average intercept of 42.36 (95% confidence interval, 41.94-42.79), an average slope of -3.53 (95% confidence interval, -3.62 to -3.44), and a mean amplification slope efficiency of 92%. This assay was linear over the concentration range of 25 to 2×10^6 copies (Fig. 1B), with a limit of detection of < 25 copies because $>95\%$ of samples at 25 copies were detected and a limit of quantitation of 25 copies because all samples were detected at that calibrator concentration. Overall plate-to-plate variability (CV) was 1%, whereas within-plate variability was $< 5\%$ at all cRNA calibrator concentrations (Table 1).

Quantification of GCC by RT-PCR in biological matrices. Linear mixed model analysis of the relationship between threshold cycle number and the amount of calibration standards spiked into total RNA isolated from tonsils yielded an average intercept of 42.67 (95% confidence interval, 38.54-48.81), an average slope of -3.46 (95% confidence interval, -4.86 to

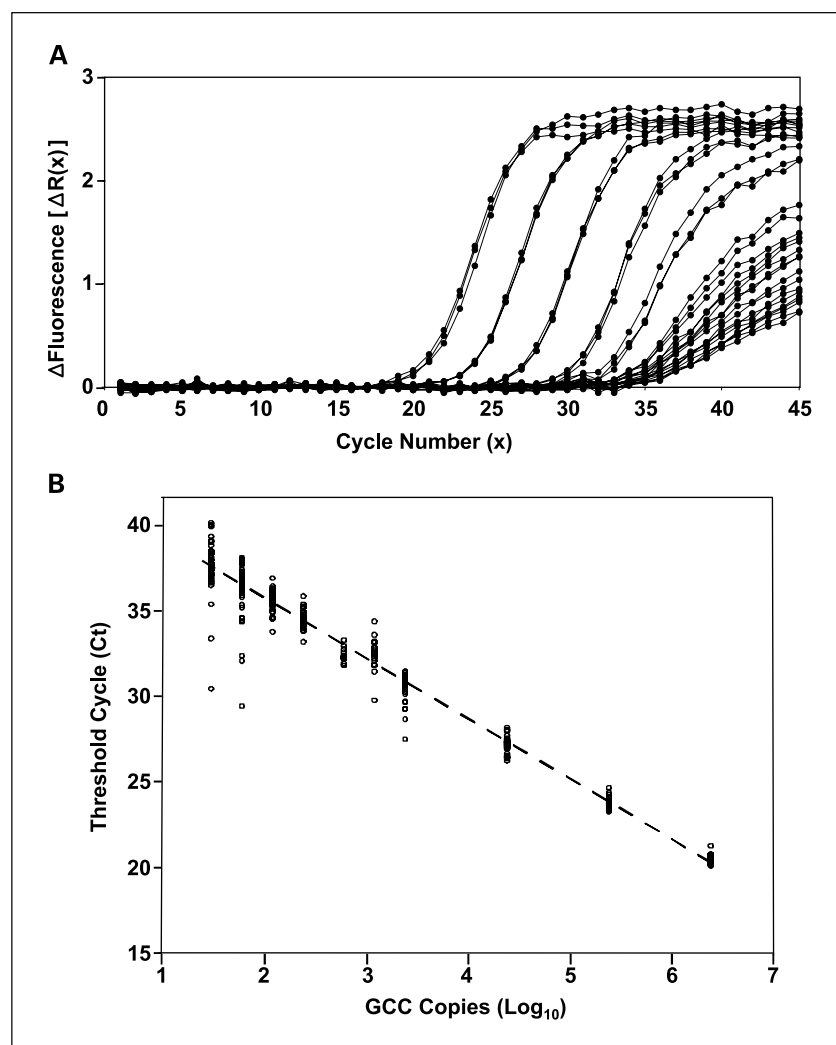


Fig. 1. qRT-PCR of GCC cRNA. *A*, inverse relationship between background-removed fluorescence $\Delta R(x)$ and cycle number x for GCC cRNA calibration standards. Calibration standards were amplified at least in duplicate. Profiles are representative of 10 separate runs done in duplicate on 5 separate plates on 5 different days. *B*, relationship between threshold cycle number (C_t) and \log_{10} concentration of GCC cRNA calibration standards. Results include all data obtained in 10 separate runs done in duplicate on 5 separate plates on 5 different days.

-2.06), and a mean amplification slope efficiency of 94%. This assay was linear over the concentration range of 50 to 2×10^6 copies with a limit of detection of <50 copies and a limit of quantitation of 50 copies. Moreover, linear mixed models of log (GCC copy number) estimated CVs of 53%, 45%, and 7% for repeat determinations of endogenous GCC expression in pathology-negative lymph nodes (background), pathology-positive lymph nodes (metastases), and primary tumors, respectively. Differences in variability in tumors and lymph nodes reflect the relative magnitude of GCC expression and the associated differences in variability at the low and high ends of calibration curves, respectively (Table 1). In the context of earlier studies validating quantification of tumor markers by RT-PCR, which showed CVs between specimens of 43% and >6,000%, the present observations show that GCC mRNA quantification by RT-PCR in relevant biological matrices employing external calibration standards is highly accurate, reproducible, and robust (28, 29).

Quantification of GCC mRNA in colorectal tumors and matched normal adjacent mucosa. GCC mRNA expression in 41 paired colorectal tumors and histologically normal adjacent mucosa was compared employing qRT-PCR and a GCC cRNA calibration curve. GCC mRNA expression varied ~2 orders of

magnitude between individuals in both normal mucosa and colorectal tumors (Fig. 2A). Further, GCC mRNA was significantly overexpressed in tumors compared with matched normal adjacent mucosa from the same patient (Fig. 2A and B). Indeed, the median GCC mRNA copy number was ~2-fold higher in tumors compared with normal mucosa ($P = 0.002$, Wilcoxon signed-rank test). Overexpression of GCC mRNA correlated closely with increased expression of GCC protein in tumors compared with normal intestinal mucosa ($P < 0.001$, exact Kruskal-Wallis test; Fig. 2C; Table 2). Moreover, altered expression of GCC is an early event in neoplastic transformation in the colon because adenoma also significantly overexpress GCC (Fig. 2C; Table 2). Although most tumor samples were moderately differentiated and from patients with Dukes stage B or C disease, GCC mRNA copy number did not obviously correlate with tumor grade or stage.

GCC mRNA estimated by qRT-PCR correlates with the presence of metastatic colorectal cancer cells in lymph nodes. RNA was extracted from 546 lymph nodes from 48 patients, including nodes with confirmed metastases (true positives) and nodes from patients with nonmalignant diseases of the colon (adenoma, familial adenomatous polyposis, Crohn's disease, and ulcerative colitis) and from sites outside the gastrointestinal

Table 1. Analytic validation of GCC standards based on five plates, two runs per plate, and replicates for each concentration

Estimate	Category	Variance	Mean C_t	CV (%)
Plate-to-plate	Overall	0.06	NA*	1.0
Within run	25 copies	2.82	37.75	4.5
Within run	50 copies	2.22	36.31	4.2
Within run	10^2 copies	0.27	35.68	1.4
Within run	2×10^2 copies	0.27	34.59	1.5
Within run	5×10^2 copies	0.06	32.46	0.8
Within run	10^3 copies	0.76	32.48	2.7
Within run	2×10^3 copies	0.63	30.47	2.7
Within run	2×10^4 copies	0.05	27.21	0.8
Within run	2×10^5 copies	0.04	23.85	0.8
Within run	2×10^6 copies	0.12	20.42	1.7

*Not applicable.

tract (true negatives; Table 3). True negative lymphoid tissues (164 lymph nodes) exhibited median GCC copy numbers <50, whereas true positive lymph nodes (15 lymph nodes) exhibited median GCC copy numbers >1,000 (Fig. 3A; Table 3). All true negative lymph nodes exhibited GCC copy numbers <400 (Fig. 3A; Table 3). In contrast, true positive lymph nodes exhibited a maximum GCC copy number of $\sim 10^5$ (Fig. 3A; Table 3). It is noteworthy that one lymph node identified as positive by histopathology was likely switched with an adjacent lymph node from the same patient that was negative by histopathology during processing, because the histologically "positive" lymph node exhibited a very low GCC copy number (<50), whereas the histologically "negative" lymph node exhibited a high GCC copy number ($>3 \times 10^4$). Evaluation of GCC mRNA expression in true positive and true negative lymph nodes by receiver-operator analysis revealed a nominal sensitivity of 93% and specificity of 97% based on a GCC RT-PCR value of ≥ 200 copies, establishing a potential threshold for the presence of occult micrometastatic disease ($n = 211$ lymph nodes; Fig. 3B). Omitting the "switched" lymph nodes yielded a threshold of 200 and a sensitivity and specificity of 100% and 97%, respectively. Application of this threshold to 367 lymph nodes from colorectal cancer patients that were free of obvious metastases by histopathology suggests that $\sim 21\%$ (76 of 367) of nodes or 26% (6 of 23) of patients might be harboring occult micrometastases by GCC qRT-PCR (Fig. 3A; Table 3). It is noteworthy that $\sim 20\%$ to 30% of patients with who are lymph node negative by histology ultimately develop recurrent disease (2–4). In that context, it is tempting to speculate that those patients that harbor occult micrometastases detected by GCC qRT-PCR are at increased risk of developing recurrent colorectal cancer (23).

Discussion

Generally, $\sim 40\%$ of patients with colorectal cancer have no evidence of disease in lymph nodes at the time of staging and are presumably cured by surgery (1). However, up to 30%

of patients with stage A disease and 50% of those with stage B disease in some series develop metastases and ultimately die (2–4). Overall, $\sim 50\%$ of patients who have undergone surgery with curative intent suffer recurrent disease. Recurrence in patients who are ostensibly disease-free presumably reflects the presence of occult micrometastases in tissues, including regional lymph nodes, undetected by current staging paradigms. The inability to detect micrometastases likely reflects methodologic limitations of histopathology. Specifically, there is a relationship between the number of lymph nodes harvested and the sensitivity of histopathologic staging, and insufficient lymph node sampling contributes to the insensitivity of current staging paradigms (9, 10). Similarly, tumor cells may distribute asymmetrically within lymph nodes (30), and evaluation of a limited number (1–2) of 10- μ m sections from lymph nodes that may be 1 cm may result in omission of key tissue sections from review. Moreover, there are limitations to the sensitivity of visual inspection, and 1 cancer cell in 200 normal cells is the lower limit for reliable histopathologic detection (11). The insensitivity of current staging paradigms presents a therapeutic dilemma to patients and physicians. Adjuvant chemotherapy has well-documented efficacy in patients with metastases in regional lymph nodes. A method that reliably quantifies tumor cells in lymph nodes that escape detection by histopathology could identify the subpopulation of patients who would benefit from adjuvant chemotherapy.

A paradigm emerging in molecular pathology is the detection of rare cells in tissues employing amplification technologies, such as RT-PCR, coupled with specific disease markers (6–8). This approach offers solutions to the methodologic limitations of histopathology. Thus, RNA can be isolated from the entire tissue specimen, permitting representative sampling of that specimen for analysis. Moreover, RT-PCR can amplify nucleic acid molecules 10^{10} -fold and detect ~ 10 mRNA molecules, which translates to the detection of a single cancer cell in $\sim 10^7$ normal cells.

Although nucleic acid amplification has the sensitivity to detect rare tumor cells in tissues, the availability of ideal molecular markers that are highly specific for colorectal cancer have lagged. In that context, GCC, the receptor for the endogenous ligands guanylin and uroguanylin and diarrheagenic bacterial heat-stable enterotoxins, is expressed selectively by intestinal epithelial cells (6–8, 19, 20). This receptor continues to be expressed following neoplastic transformation and GCC mRNA has been identified in all colorectal tumors examined regardless of the anatomic location or grade of the tumor (6–8, 19–23). However, this receptor is not expressed by normal tissues or tumors originating outside the gastrointestinal tract (6–8, 19–23). The uniformity of expression of this receptor by human colorectal tumors and its absence from other human tissues and tumors suggests that this receptor may fulfill the criteria for a highly specific molecular marker for occult micrometastases (12). Indeed, in a retrospective analysis, GCC RT-PCR detected the presence of occult micrometastases in lymph nodes from $\sim 50\%$ of 21 patients with colorectal cancer, which correlated closely with the risk of developing tumor recurrence (23).

These observations suggest that GCC may have utility for detecting occult micrometastases in patients undergoing staging for colorectal cancer. However, an assay to quantify GCC mRNA in tissues by RT-PCR has not been developed or

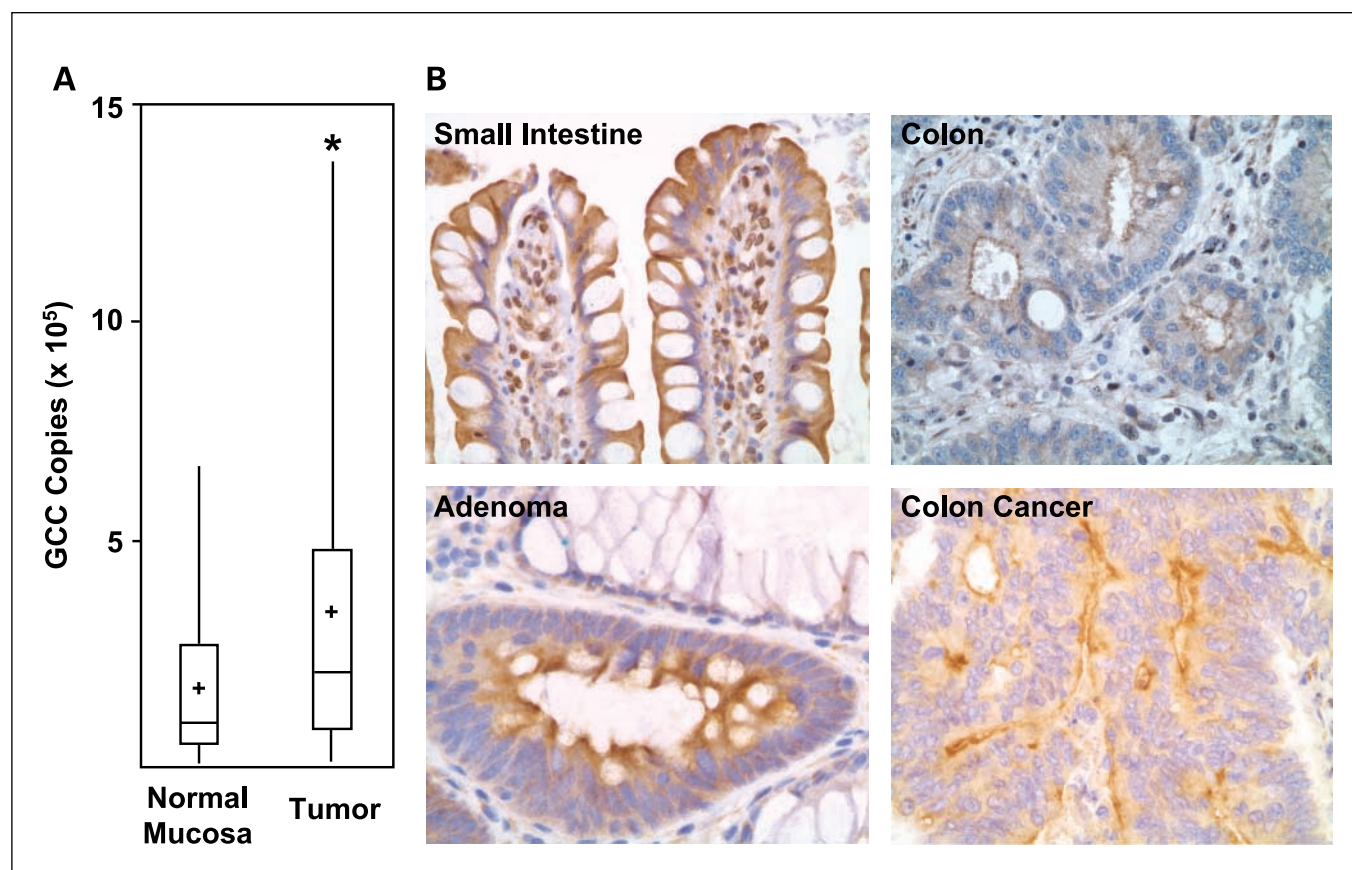


Fig. 2. GGC is overexpressed by colorectal tumors compared with normal mucosa. *A*, box and whiskers plot comparing the expression of GGC mRNA, expressed as GGC copy number/ μ g total RNA, in tumors and matched normal adjacent mucosa. Boxes, values included in 25% to 75% of the values; whiskers, extreme values; horizontal lines, median; +, mean. *, $P = 0.002$, Wilcoxon signed-rank test. *B*, GGC protein is overexpressed in colorectal tumors compared with normal intestinal mucosa. Specimens were stained with rabbit polyclonal antibodies to human GGC and staining intensity quantified employing a modification of the McCarty scoring system (18, 27). GGC protein is overexpressed in adenoma ($n = 26$) and colorectal tumors ($n = 46$) compared with normal colonic mucosa ($n = 24$; $P < 0.001$, exact Kruskal-Wallis test). Small bowel ($n = 10$) was included as a positive control.

undergone analytic or clinicopathologic validation. Here, a RT-PCR assay for quantifying GGC mRNA in tissues was developed employing GGC cRNA calibrator standards. This assay exhibited analytic characteristics that suggest its suitability for application to quantifying GGC mRNA in clinical samples. Thus, mean reaction efficiencies of this assay were >90%, which compares favorably with other validated qRT-PCR assays (29, 31). Additionally, the assay is extremely robust and can quantify GGC mRNA >6 orders of magnitude with interday and intraday variabilities <5%, reflecting a level of analytic precision superior to many validated analytic assays. Further, the assay is sensitive and can reliably quantify 25 copies of GGC mRNA. Moreover, the assay is unaffected by the biological matrix in which the target mRNA resides.

In addition to analytic performance, this assay exhibited superior clinicopathologic characteristics that suggest its utility for quantifying occult tumor cells in lymph nodes of patients undergoing staging for colorectal cancer. Thus, this assay quantified the presence of GGC in 100% of specimens of normal intestinal mucosa and colorectal tumor examined, confirming the uniformity of GGC expression in colorectal tumorigenesis (12, 18–20, 22). Further, application of this assay to 164 lymph nodes obtained from patients who do not have colorectal cancer (true negatives) established a working range of

basal GGC expression. Importantly, the range of basal expression of GGC mRNA in true negative lymph nodes could be clearly differentiated from the range of expression of that analyte in lymph nodes harboring tumor metastases visualized by histopathology. Moreover, employing those results, receiver-operator analysis revealed that GGC qRT-PCR was 100%

Table 2. Quantitation of GGC in apical membranes of normal intestinal mucosa, adenomas, and colorectal tumors by immunohistochemistry

	Intensity of apical staining			
	1+	2+	3+	Mean
Small intestine ($n = 10$) [‡]	0	7	3	2.3 [†]
Normal colon ($n = 46$) [‡]	14	31	1	1.5
Adenoma ($n = 26$)	0	8	18	2.7 [†]
Colon carcinoma ($n = 24$)	0	4	20	2.8 [†]

[‡]Includes sections from duodenum and ileum.

[†] $P < 0.001$, compared with normal colon by the exact Kruskal-Wallis test.

[‡]Normal colonic tissue adjacent to adenoma or adenocarcinoma.

sensitive and 97% specific for identifying metastatic colorectal cancer cells in lymph nodes, comparable with commercially available diagnostic tests. Taken together, the favorable analytic and clinicopathologic characteristics of the GCC qRT-PCR assay suggest its suitability for examining the utility of GCC as a marker for staging patients with colorectal cancer.

RT-PCR and immunohistochemistry confirmed overexpression of GCC in colorectal tumors compared with normal mucosa from patients (18). Increased expression in tumors underscores an emerging paradigm concerning the role of GCC in mechanisms underlying colorectal carcinogenesis. GCC signaling induced by its endogenous ligands guanylin and uroguanylin regulates the proliferation of intestinal epithelial cells by restricting transit through the cell cycle in the absence of apoptosis or necrosis (32, 33). Indeed, this signaling mechanism regulates the proliferation of epithelial cells along the crypt-villus axis in intestinal mucosa. Further, oral administration of uroguanylin suppresses adenoma formation in APC^{Min/-} mice, a murine model of intestinal carcinogenesis (34). Moreover, guanylin and uroguanylin are the genes most commonly lost during intestinal carcinogenesis in humans (35). Together, these observations suggest a model wherein GCC is a key regulator of epithelial cell proliferation along the crypt-villus axis whose dysregulation through loss of ligand expression contributes to hyperproliferation associated with neoplastic transformation (33). In that context, overexpression of GCC in tumors compared with normal mucosa reflects the plasticity of cellular compensatory responses to reduced autocrine/paracrine regulation of the cell cycle by GCC ligands, which invariably accompanies neoplastic transformation in the colon.

In summary, an assay to detect occult micrometastases, employing GCC, a specific marker for colorectal cancer cells, and qRT-PCR employing external calibration standards was developed. Analytic validation showed that this assay was robust, with high efficiency, minimum variability, high precision, and high sensitivity. In addition, clinicopathologic validation employing true positive and true negative lymph nodes showed that this assay discriminated lymph nodes free of disease from those harboring tumor cells, with high sensitivity

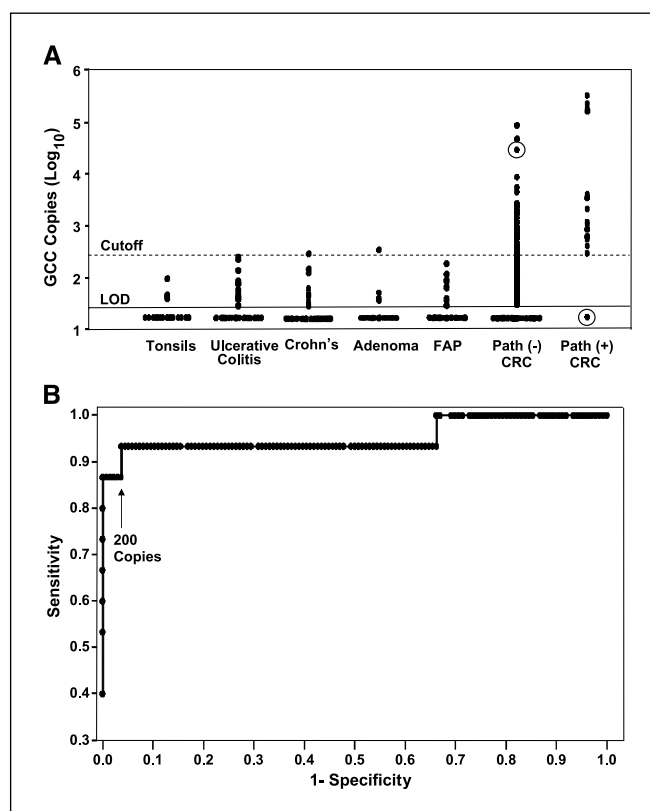


Fig. 3. GCC mRNA expression in lymph nodes. *A*, quantification of GCC mRNA in lymph nodes from patients without neoplasms or from those with colorectal cancer. Tonsils were obtained from individuals undergoing tonsillectomy. In some cases, lymph nodes were obtained from patients with nonmalignant diseases of the intestine (true negatives), including ulcerative colitis, Crohn's disease, adenomatous hyperplasia, or familial adenomatous polyposis (*FAP*). In addition, lymph nodes were obtained from patients with colorectal cancer, which harbored tumor metastases visualized by histopathology [true positives; *Path (+) CRC*]. Further, lymph nodes were obtained from patients with colorectal cancer that were free of metastases by histopathology [*Path (-) CRC*]. Solid horizontal line, limit of detection (*LOD*) of the assay in biological matrix (50 copies); dashed horizontal line, cutoff value estimated from receiver-operator analysis (see *B*) for identifying lymph nodes harboring micrometastases (200 copies). Values circled were presumably switched at the time of analysis. *B*, receiver-operator analysis of GCC mRNA expression in true positive and true negative lymph nodes. This analysis estimates a threshold for the presence of occult micrometastases of 200 copies, with a nominal sensitivity of 93% and a specificity of 97%.

Table 3. GCC expression estimated by qRT-PCR in 546 lymph nodes from 48 patients

Lymph nodes	Median	Minimum	Maximum
Extraintestinal (<i>n</i> = 20)	<50	<50	95
Ulcerative colitis (<i>n</i> = 40)	<50	<50	255
Crohn's disease (<i>n</i> = 34)	<50	<50	309
Adenoma (<i>n</i> = 23)	<50	<50	369
Familial adenomatous polyposis (<i>n</i> = 42)	<50	<50	186
Other cancers (<i>n</i> = 5)	<50	<50	<50
Colorectal cancer			
Pathology (-), (<i>n</i> = 367)	85	<50	86,178
Pathology (+), (<i>n</i> = 15)	1,183	<50*	323,167

*Includes true negative lymph node inadvertently switched with true positive lymph node (see Results).

and specificity. Importantly, applying this assay to lymph nodes from colorectal cancer patients, which were free of metastases by histopathology, suggested that a significant fraction of those patients harbor occult micrometastases. This assay will be applied to the analysis of ~10,000 lymph nodes in an ongoing prospective multi-institutional trial to define the sensitivity and specificity of GCC qRT-PCR for staging patients with colorectal cancer (12). Specifically, this trial will define the utility of GCC qRT-PCR to prospectively identify patients at increased risk for developing recurrent colorectal cancer who might otherwise benefit from receiving adjuvant chemotherapy. In that context, the clinicopathologic threshold established here for the presence of occult micrometastases illustrates the proof-of-concept for the discriminatory utility of GCC qRT-PCR. Ultimately, that threshold will be defined by clinical outcomes, including disease recurrence and disease-free survival, rather than a histopathologic end point visualizing cancer cells.

References

1. Jemal A, Tiwari RC, Murray T, et al. Cancer statistics, 2004. *CA Cancer J Clin* 2004;54:8–29.
2. Greene FL, Balch CM, Fleming ID, et al. *AJCC cancer staging handbook*, 6th ed. New York: Springer; 2002.
3. O'Connell JB, Maggard MA, Ko CY. Colon cancer survival rates with the new American Joint Committee on Cancer sixth edition staging. *J Natl Cancer Inst* 2004;96:1420–5.
4. Meyerhardt JA, Mayer RJ. Systemic therapy for colorectal cancer. *N Engl J Med* 2005;352:476–87.
5. International Multicentre Pooled Analysis of B2 Colon Cancer Trials (IMPACT B2) Investigators. Efficacy of adjuvant fluorouracil and folinic acid in B2 colon cancer. *J Clin Oncol* 1999;17:1356–63.
6. Lugo TG, Braun S, Cote RJ, Pantel K, Rusch V. Detection and measurement of occult disease for the prognosis of solid tumors. *J Clin Oncol* 2003;21:2609–15.
7. Pantel K. Detection of minimal disease in patients with solid tumors. *J Hematother* 1996;5:359–67.
8. Pantel K, Cote RJ, Fodstad O. Detection and clinical importance of micrometastatic disease. *J Natl Cancer Inst* 1999;91:1113–24.
9. Baxter NN, Virnig DJ, Rothenberger DA, Morris AM, Jessurun J, Virnig BA. Lymph node evaluation in colorectal cancer patients: a population-based study. *J Natl Cancer Inst* 2005;97:219–25.
10. Le Voyer TE, Sigurdson ER, Hanlon AL, et al. Colon cancer survival is associated with increasing number of lymph nodes analyzed: a secondary survey of Intergroup Trial INT-0089. *J Clin Oncol* 2003;21:2912–9.
11. Ratto C, Sofo L, Ippoliti M, et al. Accurate lymph-node detection in colorectal specimens resected for cancer is of prognostic significance. *Dis Colon Rectum* 1999;42:143–54; discussion 54–8.
12. Frick GS, Pitari GM, Weinberg DS, Hyslop T, Schulz S, Waldman SA. Guanylyl cyclase C: a molecular marker for staging and postoperative surveillance of patients with colorectal cancer. *Expert Rev Mol Diagn* 2005;5:701–13.
13. Bernard PS, Wittwer CT. Real-time PCR technology for cancer diagnostics. *Clin Chem* 2002;48:1178–85.
14. Bustin SA, Mueller R. Real-time reverse transcription PCR (qRT-PCR) and its potential use in clinical diagnosis. *Clin Sci (Lond)* 2005;109:365–79.
15. Lacroix J, Doeberitz MK. Technical aspects of minimal residual disease detection in carcinoma patients. *Semin Surg Oncol* 2001;20:252–64.
16. Mocellin S, Rossi CR, Pilati P, Nitti D, Marincola FM. Quantitative real-time PCR: a powerful ally in cancer research. *Trends Mol Med* 2003;9:189–95.
17. Lucas KA, Pitari GM, Kazerounian S, et al. Guanylyl cyclases and signaling by cyclic GMP. *Pharmacol Rev* 2000;52:375–414.
18. Birbe R, Palazzo JP, Walters R, Weinberg D, Schulz S, Waldman SA. Guanylyl cyclase C is a marker of intestinal metaplasia, dysplasia, and adenocarcinoma of the gastrointestinal tract. *Hum Pathol* 2005;36:170–9.
19. Carrithers SL, Barber MT, Biswas S, et al. Guanylyl cyclase C is a selective marker for metastatic colorectal tumors in human extraintestinal tissues. *Proc Natl Acad Sci U S A* 1996;93:14827–32.
20. Carrithers SL, Parkinson SJ, Goldstein S, Park P, Robertson DC, Waldman SA. *Escherichia coli* heat-stable toxin receptors in human colonic tumors. *Gastroenterology* 1994;107:1653–61.
21. Chen G, McIver CM, Texler M, et al. Detection of occult metastasis in lymph nodes from colorectal cancer patients: a multiple-marker reverse transcriptase-polymerase chain reaction study. *Dis Colon Rectum* 2004;47:679–86.
22. Steinbrecher KA, Mann EA, Giannella RA, Cohen MB. Increases in guanylin and uroguanylin in a mouse model of osmotic diarrhea are guanylate cyclase C-independent. *Gastroenterology* 2001;121:1191–202.
23. Cagir B, Gelmann A, Park J, et al. Guanylyl cyclase C messenger RNA is a biomarker for recurrent stage II colorectal cancer. *Ann Intern Med* 1999;131:805–12.
24. Bustin SA. Quantification of mRNA using real-time reverse transcription PCR (RT-PCR): trends and problems. *J Mol Endocrinol* 2002;29:23–39.
25. Bustin SA. Absolute quantification of mRNA using real-time reverse transcription polymerase chain reaction assays. *J Mol Endocrinol* 2000;25:169–93.
26. Bustin SA, Benes V, Nolan T, Pfaffl MW. Quantitative real-time RT-PCR—a perspective. *J Mol Endocrinol* 2005;34:597–601.
27. McCarty KS, Jr., Miller LS, Cox EB, Konrath J, McCarty KS, Sr. Estrogen receptor analyses. Correlation of biochemical and immunohistochemical methods using monoclonal anti-receptor antibodies. *Arch Pathol Lab Med* 1985;109:716–21.
28. Bustin SA, Gyselman VG, Williams NS, Dorudi S. Detection of cytokeratins 19/20 and guanylyl cyclase C in peripheral blood of colorectal cancer patients. *Br J Cancer* 1999;79:1813–20.
29. Slack JL, Bi W, Livak KJ, et al. Pre-clinical validation of a novel, highly sensitive assay to detect PML-RAR α mRNA using real-time reverse-transcription polymerase chain reaction. *J Mol Diagn* 2001;3:141–9.
30. Abrahamsen HN, Sorensen BS, Nexø E, Hamilton-Dutoit SJ, Larsen J, Steiniche T. Pathologic assessment of melanoma sentinel nodes: a role for molecular analysis using quantitative real-time reverse transcription-PCR for MART-1 and tyrosinase messenger RNA. *Clin Cancer Res* 2005;11:1425–33.
31. Cassinat B, Zasadowski F, Balitrand N, et al. Quantitation of minimal residual disease in acute promyelocytic leukemia patients with t(15;17) translocation using real-time RT-PCR. *Leukemia* 2000;14:324–8.
32. Pitari GM, Di Guglielmo MD, Park J, Schulz S, Waldman SA. Guanylyl cyclase C agonists regulate progression through the cell cycle of human colon carcinoma cells. *Proc Natl Acad Sci U S A* 2001;98:7846–51.
33. Pitari GM, Zingman LV, Hodgson DM, et al. Bacterial enterotoxins are associated with resistance to colon cancer. *Proc Natl Acad Sci U S A* 2003;100:2695–9.
34. Shailubhai K, Yu HH, Karunanandaa K, et al. Uroguanylin treatment suppresses polyp formation in the Apc(Min/+) mouse and induces apoptosis in human colon adenocarcinoma cells via cyclic GMP. *Cancer Res* 2000;60:5151–7.
35. Notterman DA, Alon U, Sierk AJ, Levine AJ. Transcriptional gene expression profiles of colorectal adenoma, adenocarcinoma, and normal tissue examined by oligonucleotide arrays. *Cancer Res* 2001;61:3124–30.

Clinical Cancer Research

A Validated Quantitative Assay to Detect Occult Micrometastases by Reverse Transcriptase-Polymerase Chain Reaction of Guanylyl Cyclase C in Patients with Colorectal Cancer

Stephanie Schulz, Terry Hyslop, Janis Haaf, et al.

Clin Cancer Res 2006;12:4545-4552.

Updated version Access the most recent version of this article at:
<http://clincancerres.aacrjournals.org/content/12/15/4545>

Cited articles This article cites 34 articles, 14 of which you can access for free at:
<http://clincancerres.aacrjournals.org/content/12/15/4545.full#ref-list-1>

Citing articles This article has been cited by 10 HighWire-hosted articles. Access the articles at:
<http://clincancerres.aacrjournals.org/content/12/15/4545.full#related-urls>

E-mail alerts [Sign up to receive free email-alerts](#) related to this article or journal.

Reprints and Subscriptions To order reprints of this article or to subscribe to the journal, contact the AACR Publications Department at pubs@aacr.org.

Permissions To request permission to re-use all or part of this article, use this link
<http://clincancerres.aacrjournals.org/content/12/15/4545>.
Click on "Request Permissions" which will take you to the Copyright Clearance Center's (CCC) Rightslink site.